

# Cloud feedbacks in extratropical cyclones: insight from long-term satellite data and high-resolution global simulations

Daniel T. McCoy<sup>1</sup>, Paul R. Field<sup>1,2</sup>, Gregory S. Elsaesser<sup>3</sup>, Alejandro Bodas-Salcedo<sup>2</sup>, Brian H. Kahn<sup>4</sup>, Mark D. Zelinka<sup>5</sup>, Chihiro Kodama<sup>6</sup>, Thorsten Mauritsen<sup>7</sup>, Benoit Vanniere<sup>8</sup>, Malcolm Roberts<sup>2</sup>, Pier L. Vidale<sup>8</sup>, David Saint-Martin<sup>9</sup>, Aurore Voldoire<sup>9</sup>, Rein Haarsma<sup>10</sup>, Adrian Hill<sup>2</sup>, Ben Shipway<sup>2</sup>, Jonathan Wilkinson<sup>2</sup>

<sup>1</sup>Institute of Climate and Atmospheric Sciences, University of Leeds, UK

<sup>2</sup>Met Office, UK

10 <sup>3</sup>Department of Applied Physics and Applied Mathematics, Columbia University and NASA Goddard Institute for Space Studies, New York, NY, USA

<sup>4</sup>Jet Propulsion Laboratory, California Institute of Technology, Pasadena, CA, USA

<sup>5</sup>Cloud Processes Research and Modeling Group, Lawrence Livermore National Laboratory, Livermore, California, USA

<sup>6</sup>Japan Agency for Marine-Earth Science and Technology, Yokohama, Japan

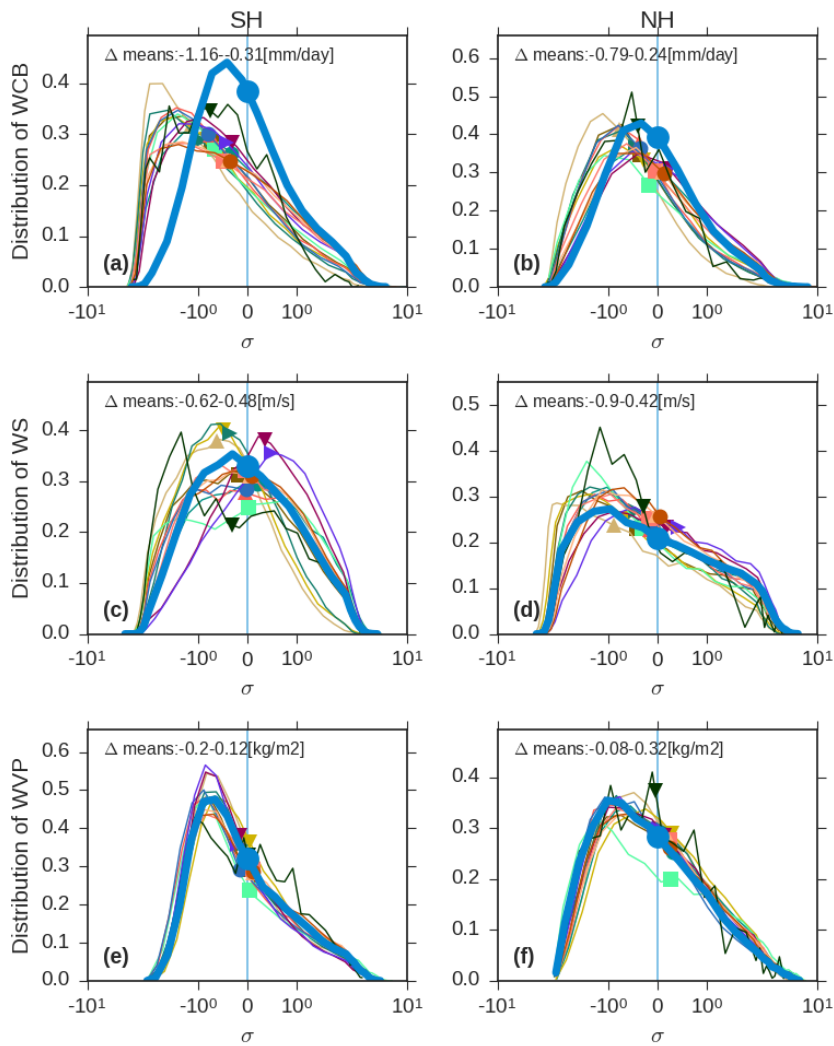
<sup>7</sup>Max Planck Institute for Meteorology, Hamburg, Germany

15 <sup>8</sup>National Centre for Atmospheric Science-Climate, Department of Meteorology, University of Reading, Reading, UK

<sup>9</sup>Centre National de Recherches Météorologiques (CNRM), Météo-France/CNRS, 42 Avenue Gaspard Coriolis, 31057 Toulouse, France

<sup>10</sup>Royal Netherlands Meteorological Institute, De Bilt, Netherlands

*Correspondence to:* Daniel T. McCoy (d.t.mccoy@leeds.ac.uk)



5 **Fig. S 1** Normalized distributions of WCB moisture flux (a,b), 10-meter wind speed(c,d), and WVP(e,f) in extratropical cyclones. SH cyclones are shown in the left column and NH cyclones are shown in the right column. Distributions are normalized by subtracting the observed mean and dividing by the observed standard deviation. Means for each GCM and for the observations are shown using markers (as in Fig. 1). The range of the difference between the observed mean and the means of individual GCMs is noted in absolute units for each hemisphere and variable.

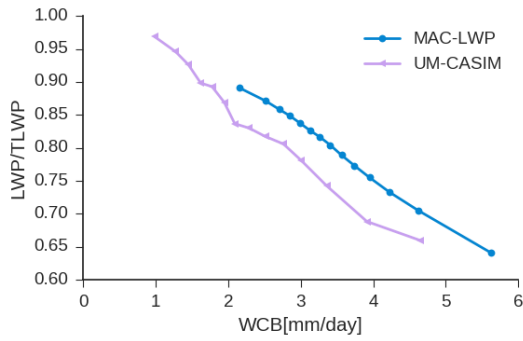
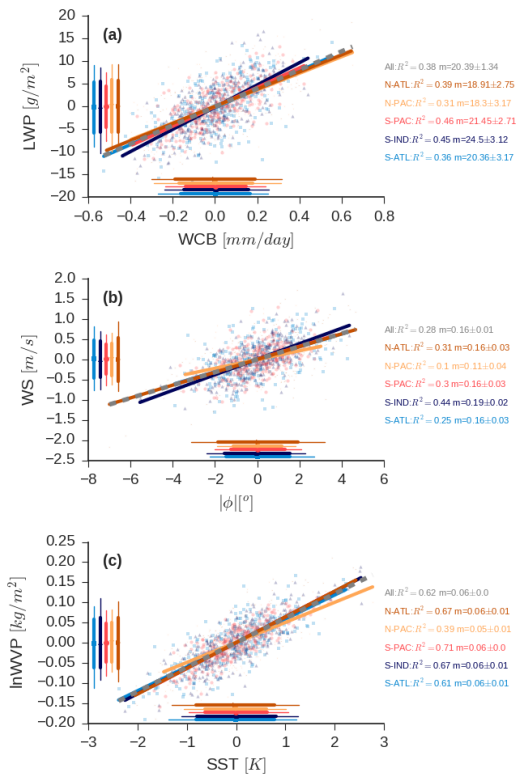


**Fig. S 2** Cyclone-mean LWP (cloud) over TLWP (cloud+rain) calculated from the MAC-LWP observations and simulated by the UM-CASIM model as a function of WCB moisture flux. Observations and models are averaged into 14 equal quantiles of WCB moisture flux for visual clarity.



5

**Fig. S 3** As in Fig. 5, but only considering extratropical cyclones centered poleward of  $35^\circ$ .

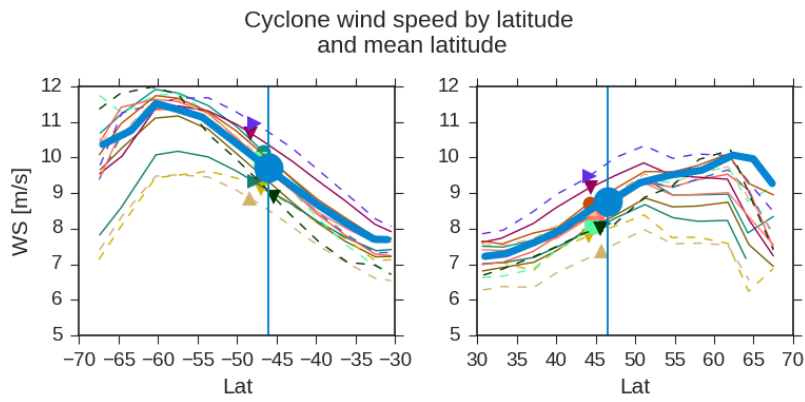
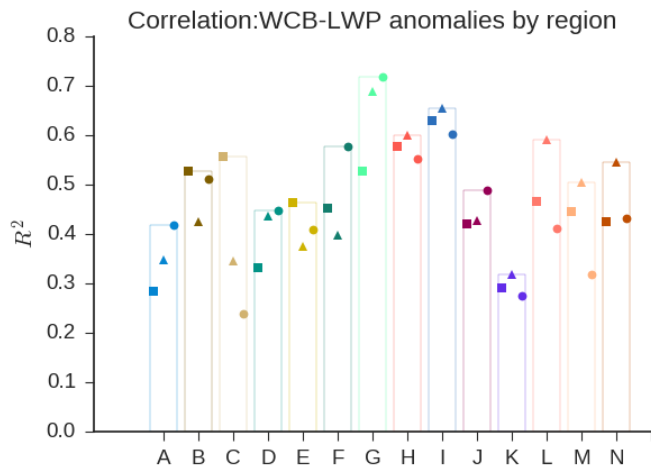
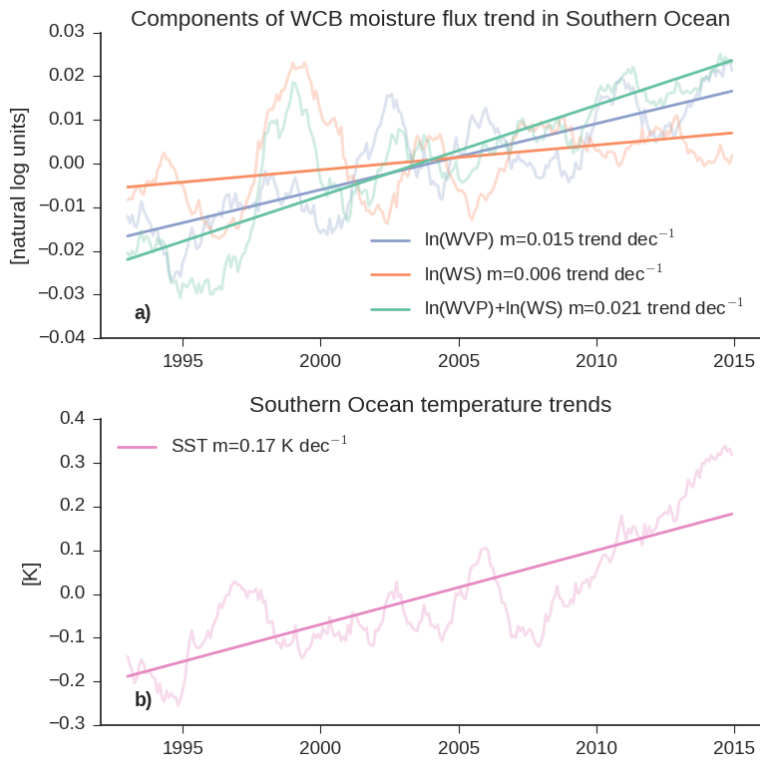


Fig. S 4 Cyclone-mean wind speed by latitude in observations (thick blue line) and models (as in Fig. 1). Markers denote mean cyclone location. Note that contributions from each month are weighted equally in the average.

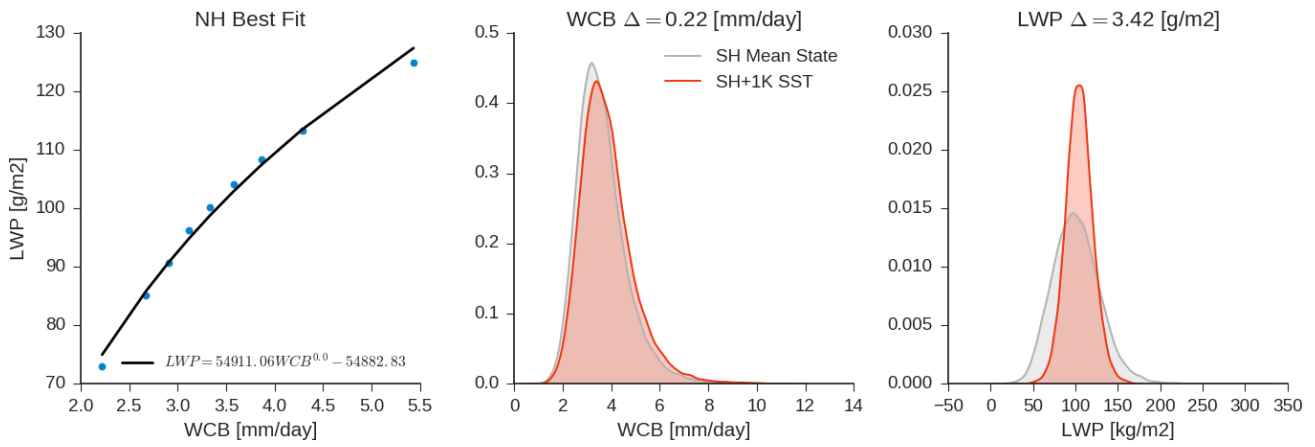


5 Fig. S 5 As in Fig. 6, but showing the  $R^2$  between WCB moisture flux and  $LWP_{RM}$  monthly-mean anomalies for each basin in the models and observations.



**Fig. S 6 Trends in various cyclone-mean quantities for cyclones centered between 44.5°S and 59.5°S. (a) Trends in the natural log of cyclone-mean wind speed, WVP, and their sum. Note that  $\ln(WCB) = \ln(k) + \ln(WS_{10m}) + \ln(WVP)$ . The trend in units of the natural log of each quantity per decade is given in the legend. Wind speed is in m/s, WVP is in kg/m<sup>2</sup>. (b) the trend in SST within cyclones.**

5



5 **Fig. S 7 (left)** The  $LWP_{CM}$  observed in NH as a function of WCB moisture flux, the best fit line to the observations using the form  $LWP_{CM} = a \cdot WCB^b + c$  is shown using a black line. The observations are binned into equal quantiles for visual clarity. **(middle)** The distribution of NH WCB moisture flux in the current climate, and when WVP moisture flux is scaled by 1.06 consistent with a uniform 1K increase in SST. The different in WCB moisture flux is noted in the title. **(right)** The distribution of  $LWP_{CM}$  in the current climate and as predicted by the best fit and scaling WVP by 1.06. The difference in LWP is noted in the title.

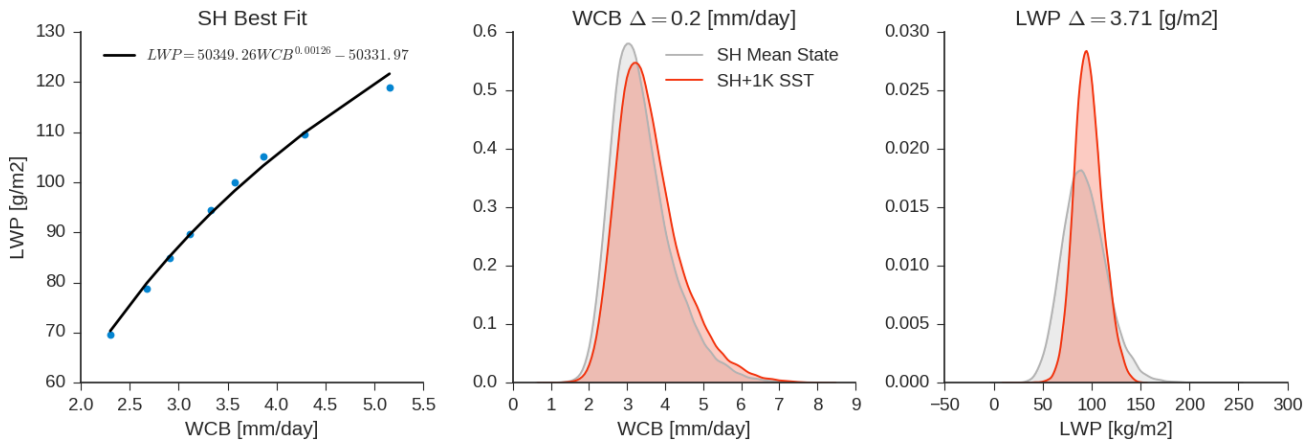


**Fig. S 8** As in Fig. S 7, but showing the SH.

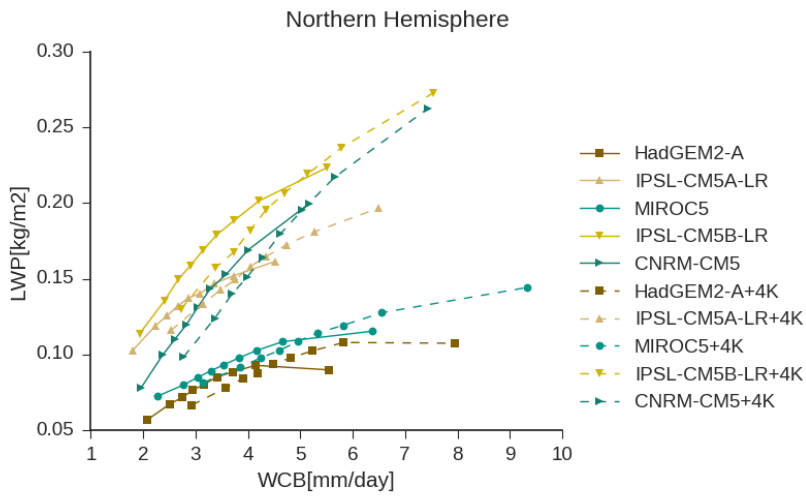


Fig. S 9 As in Fig. 8, but showing the NH.

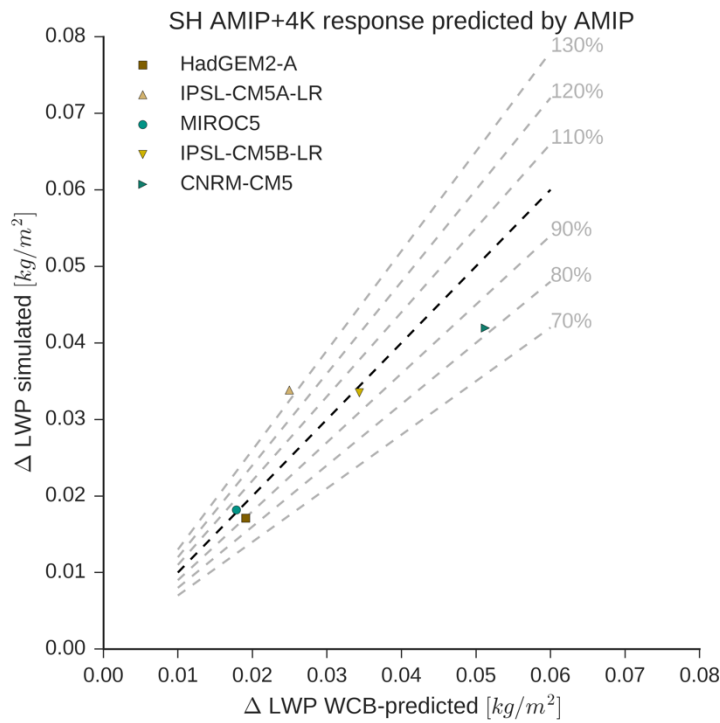


Fig. S 10 The difference in cyclone LWP in the SH between AMIP and AMIP+4K simulations versus the difference in SH cyclone LWP inferred from changes in WCB moisture flux and the relationship between WCB moisture flux and LWP<sub>CM</sub> in the current climate. The one to one line is shown as a dark dashed line.

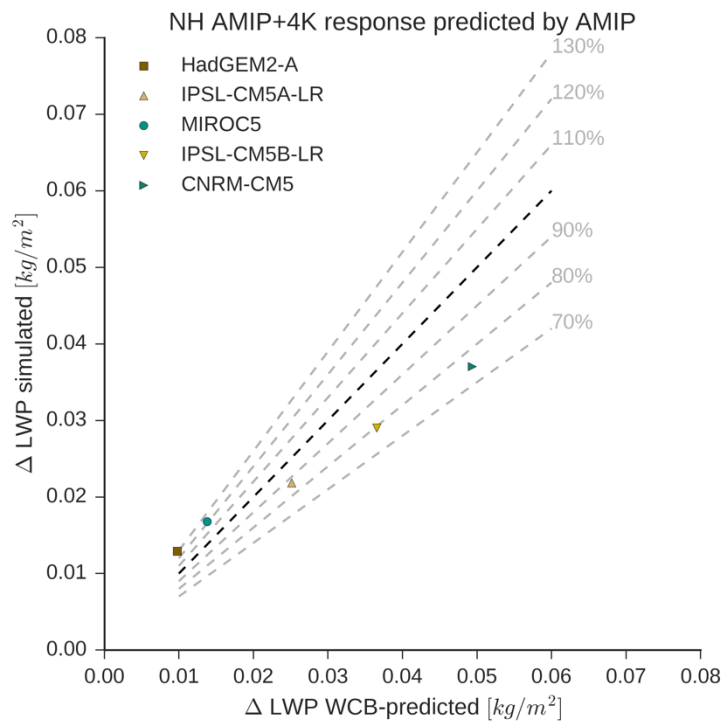


Fig. S 11 As in Fig. S 10, but showing the NH.

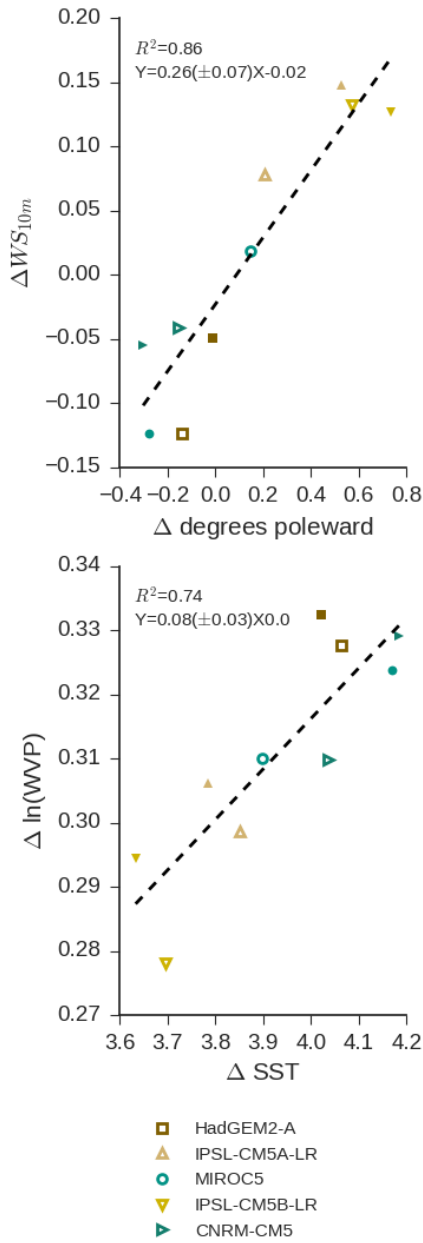
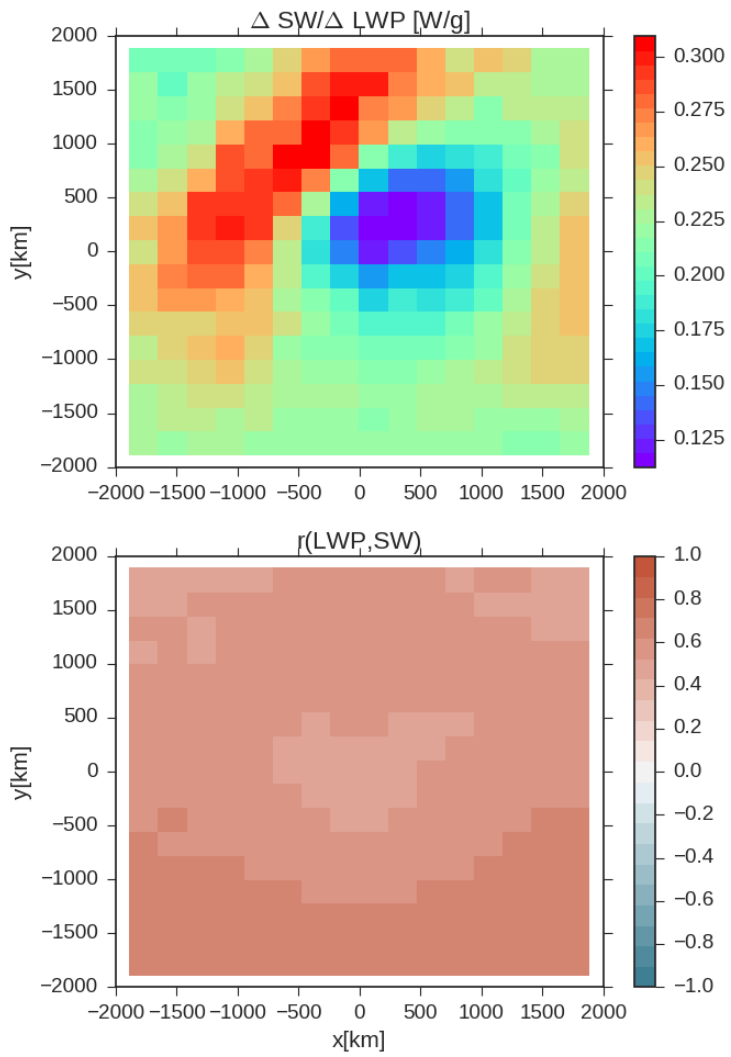
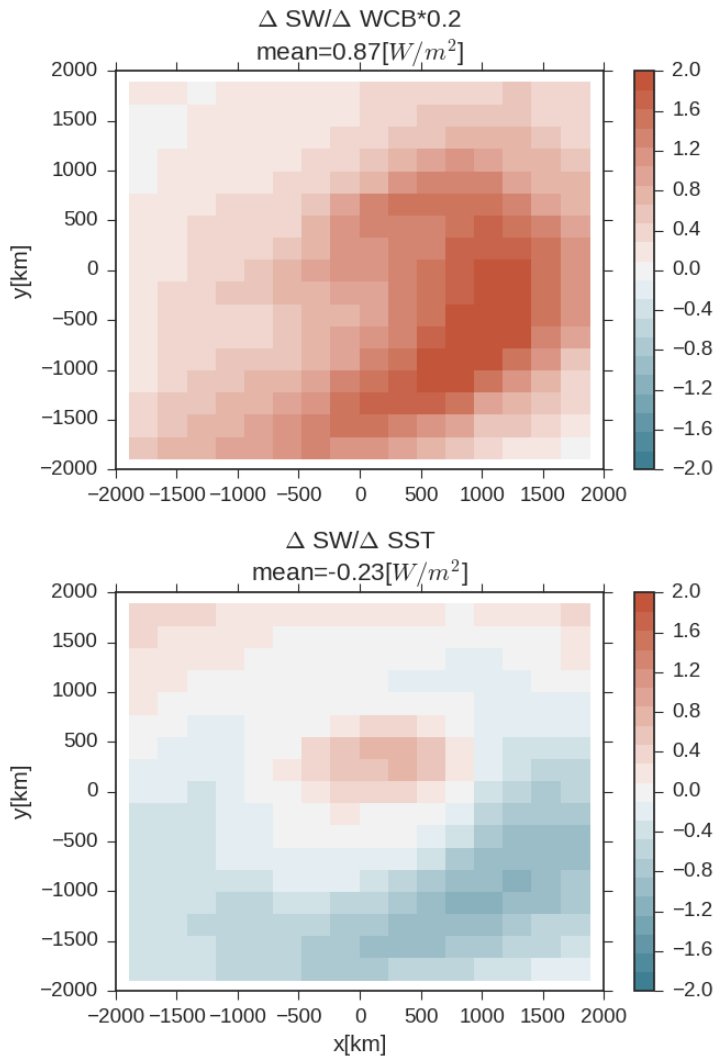


Fig. S 12 Changes in cyclone-mean wind speed at 10m ( $WS_{10m}$ ) and the natural log of WVP between AMIP and AMIP+4K simulations plotted against changes in mean poleward cyclone latitude and SST, respectively. Open symbols show the change over the NH and closed symbols show the change over the SH. The best fit line to NH and SH is noted in each plot along with 95% confidence in the slope.

5



**Fig. S 13** The regression coefficient relating changes in reflected shortwave (SW) to perturbations in  $LWP_{ij}$  across the cyclone composite (top). The correlation between variability in  $LWP_{ij}$  and reflected shortwave (bottom).



**Fig. S 14** The change in reflected shortwave (SW) within SH cyclones implied by a 0.2 mm/day increase in WCB moisture flux (top) and a 1K increase in SST (bottom). The change is calculated as the product of the coefficient relating shortwave to LWP (Fig. S 13) and Fig. 9cd.

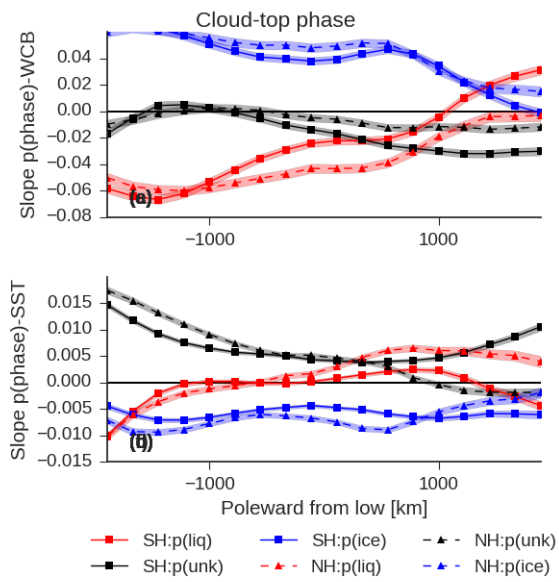


Fig. S 15 As in Fig. 9 and Fig. 10, but showing the multiple linear regression slopes relating phase to  $SST_{ij}$  and WCB moisture flux for both hemispheres and zonally-averaged. (a) shows the coefficient relating cloud top phase to the WCB moisture flux into the cyclone. (b) shows the coefficient relating cloud top phase to  $SST_{ij}$  variability.

5